Available online at www.sciencedirect.com

SCIENCE DIRECT®

Journal of Controlled Release 98 (2004) 367–378

journal of controlled release

www.elsevier.com/locate/jconrel

Time and depth resolved visualisation of the diffusion of a lipophilic dye into the hair follicle of fresh unfixed human scalp skin

Ylva Y. Grams[a], Lynne Whitehead[b], Paul Cornwell[b], Joke A. Bouwstra[a,*]

[a] *Leiden/Amsterdam Centre for Drug Research, Department of Pharmaceutical Technology, Leiden University, P.O. Box 9502, Einsteinweg 55, 2300 RA Leiden, The Netherlands*

[b] *Unilever Research Port Sunlight, Quarry Road East, Bebington, Wirral L63 3JW, UK*

Received 6 January 2004; accepted 17 May 2004
Available online 2 July 2004

Abstract

Visualising the penetration pathway of a lipophilic model dye into the hair follicle of fresh unfixed human skin would facilitate optimisation of drug formulations for local delivery to the pilosebaceous unit. A block of fresh human scalp skin was mechanically fixed in a newly designed combination of cutting device/on-line diffusion cell, manual cross-sectioned perpendicular to the skin surface and sealed to create the donor and acceptor compartment. The donor phase consisted of a saturated solution of Bodipy® FL C_5 in a citric acid buffer solution. Images were obtained on-line by confocal laser scanning microscopy (CLSM) every 30 min for 16 h. For each time point and each skin region relative intensity values were calculated. The on-line visualisation showed a fast diffusion of the label into the gap of the hair follicle followed by a fluorescent staining in the gap itself. The data strongly indicate that the fluorescence in the cuticle originates mainly from the dye of the gap and not from the surrounding epidermis. The on-line visualisation provides a new and excellent tool to monitor simultaneous changes in distribution profiles in the various skin layers including the hair follicle. This information can be used to determine penetration pathways in the skin.

Keywords: On-line diffusion; Human skin; Hair follicle; Visualisation

1. Introduction

Investigation of the hair follicle as a local target is of special interest for pharmaceutical and cosmetic applications with regard to treatment of skin diseases and improvement of the hair condition. Optimised local targeting would decrease the necessary amount of the active drug in the formulation and has the potential to decrease toxicity. Additionally gene delivery to local targets would be feasible.

Several techniques have been applied to study the deposition of a penetrant in the follicular regions. These techniques have been summarised by Lauer et al. [1], Touitou et al. [2], Corcuff and Pierard [3].

* Corresponding author. Tel.: +31-71-527-4208; fax: +31-71-527-4565.
E-mail address: bouwstra@chem.leidenuniv.nl (J.A. Bouwstra).

0168-3659/$ - see front matter © 2004 Published by Elsevier B.V.
doi:10.1016/j.jconrel.2004.05.010

Most of the techniques include fixation of the skin by freezing or embedding followed by slicing into thin sections and visualisation. During these procedures artefact formation due to cell damaging and delocalisation of the substance might occur. Additionally visualisation of diffusion processes *on-line* is impossible once the skin is fixated. Chemical fixation of the skin is unnecessary in conventional confocal laser scanning microscopy (CLSM) and confocal Raman spectroscopy combined with confocal microscopy [4] and thereby enables the use of fresh skin. CLSM in combination with optical sectioning allows the visualisation of depth profiles reaching the epidermal–dermal junction [5] in vitro [6–10]. More recently new microscopic techniques have been developed taking advantage of reflected light, which can be used for in vivo real-time visualisation of non-stained skin [11] reaching similar depth levels [12–19]. These visualisation techniques of the skin have been reviewed by Cullander [20].

When fluorophores are used to investigate diffusion processes by CLSM, scattering and re-absorption of emitted fluorescence limits the possibility of intensity comparison between different depths. A manual cross-section perpendicular to the skin surface preceding the visualisation circumvents this problem and allows the visualisation of the fluorophore in epidermis and dermis in one image. Most importantly, since the epidermis and the dermis (*z*-direction) are imaged at identical depths parallel to the cross-section, the fluorescence distribution can therefore be determined in a relative manner [21,22]. This cross-sectional imaging has previously been extended by Grams et al. [23] to resolve for the first time the visualisation of the diffusion of a model penetrant into non-fixed fresh skin on-line. That study has been focussed on the visualisation of diffusion processes in the epidermis and the upper part of the dermis.

The aim of the present study is to visualise the diffusion process of a model dye *on-line* into the upper part of the hair follicle in real time and in depth. Images of the diffusion process were taken every 30 min for a period of 16 h. Changes in intensity distribution in time are of interest and might provide information regarding the follicular contribution to the diffusion process in vitro.

2. Materials and methods

2.1. Materials

Bodipy® FL C_5 was obtained from Molecular Probes, The Netherlands. Fresh human scalp skin (aged 45–66 years, mostly female) from cosmetic face lift surgery was transported on filter paper soaked with phosphate buffered saline pH 7.4 (139 mM NaCl, 2.5 mM KCl, 8 mM Na_2HPO_4, 1.5 mM KH_2PO_4, 25 mg/l streptomycin and 25000 U/l penicillin) and stored at 4 °C until used. Within 4 h after face-lift surgery, the experiment was started thereby avoiding alteration of the skin due to extended storage and freezing. Results of skin from three different donors was used. The dental clay Impregum F (Espe) for sealing of the on-line diffusion cell was purchased from Dental Union BV, The Netherlands.

2.2. Methods

2.2.1. Preparation for the diffusion experiment

The acceptor phase consisted of phosphate buffered saline pH 7.4, with the same buffer composition as has already been used for transport and storage. The donor phase consisted of saturated solution (0.1 mg/ml) of Bodipy® FL C_5 (excitation/emission = 505/511 nm) in 50 mM citric acid buffer (CAB) at a pH of 5.0, equivalent to that of the skin surface.

Upon arrival in our laboratory, the scalp skin was gently cleaned with tissue and the surface was wiped with PBS followed by 70% ethanol to remove any contaminants of the subcutaneous fat from the skin surface. The hair was cut with surgical scissors to a length of 2 mm above the surface. Subsequently a skin square of 8 × 8 mm with the hair follicles parallel to two sides of the square is cut with a stanza for later use. The skin square included the epidermis (viable and non-viable), dermis and subcutaneous fat.

2.2.2. Preparation of the on-line diffusion cell

Previously the preparation of the on-line diffusion cell has been described in detail [23]. This cell has been prepared by the Fine Mechanical Department of the Leiden/Amsterdam Centre for Drug Research, Leiden. Basically, the on-line diffusion cell is part of a combined cutting device/on-line diffusion cell. The skin block is mounted into the cutting device with the

stratum corneum being supported by a silicone square to avoid artefact formation during sectioning. After mechanical fixation the skin is cut from the dermis side to the stratum corneum side resulting in a flat cross-sectional cutting plane with the acceptor compartment at the dermis side. Subsequently the donor compartment is screwed onto the mechanically fixed skin with the acceptor compartment. In order to seal donor and acceptor compartments and to prevent any leakage along the cutting plane, the on-line diffusion cell is completed by fixing a pioloform-coated (0.5% (w/v) pioloform in chloroform) cover glass with dental clay (Impregum F) to the diffusion compartments. The dental clay seal allows injection of the acceptor and donor phase at the start of the experiment. A schematic drawing of the on-line diffusion cell is provided in Fig. 1A. A more detailed explanation is provided in our recent publication [23].

2.2.3. Image acquisition using CLSM

The confocal microscope was a Bio-Rad MRC 600 set-up, equipped with a argon/HeNe laser with an excitation wavelength of 488 nm. The microscopic unit was an inverted Zeiss IM-35 with a PlanApo 20 and PlanApo 60 objective. Fixed microscopic settings of the CLSM were used and determined in pilot experiments. At these fixed settings autofluorescence did not interfere with our measurements. However autofluorescence was visible at the most sensitive settings, which is an essential tool for the location of the hair follicle prior to the application of the donor phase. A hair follicle, which can be analysed, has to emerge from the skin a few micrometers below the cutting plane however at sufficient distance to avoid visualisation of damaged cells due to the mechanical cutting procedure.

After injection of the donor phase into the equivalent compartment, images were collected every 30 min starting 10 min after application for a period of 16 h. Possible leakage of donor phase between the cover glass and cross-section plane of the skin has previously been studied. If there was evidence for leakage, the study has been excluded from further investigation. When swelling of the skin appeared to have a severe

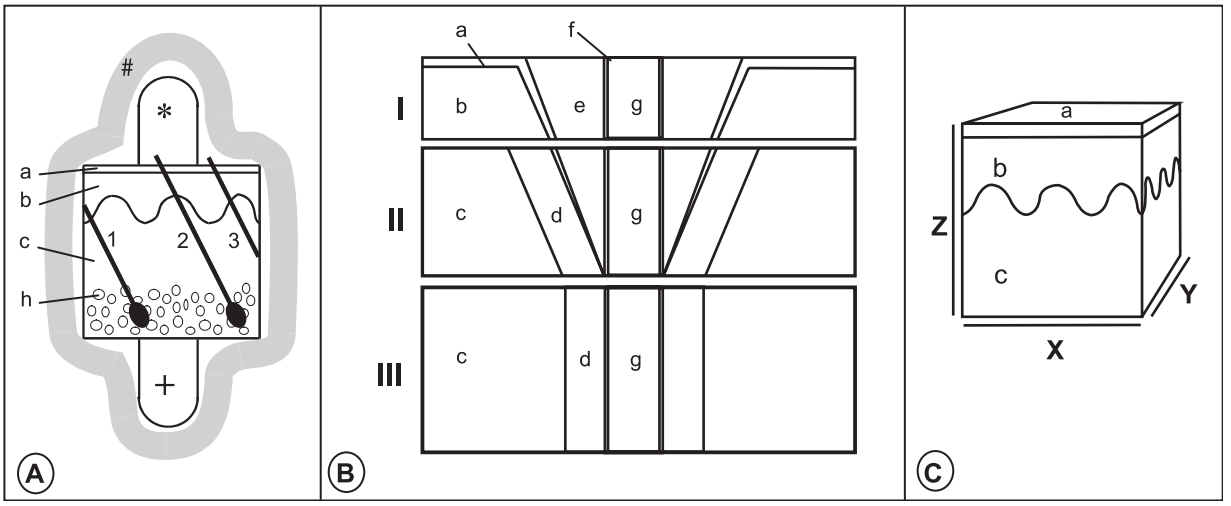

Fig. 1. (A) View of cross-section with donor compartment (*), acceptor compartment (+), stratum corneum (a), epidermis (b), dermis (c), subcutaneous fat (h) and hair follicles (1–3) sealed with dental clay (#). Hair follicles 1 and 3 do not have access to the donor phase. Therefore only hair follicle 2 can be investigated. Images B and C depict the model skin block from which the volumes of the selected skin areas have been calculated. (C) The overall dimensions of the model skin block were 400 μm on all three sides (x, y, z). The model block contained the stratum corneum (a), the viable epidermis (b), the dermis (c) and 260 hair follicles per cm^2. (B) X–z view displaying the subdivision in the various skin areas: stratum corneum (a), the viable epidermis (b), the dermis (c), outer root sheath (d), gap (e), cuticle (f) and hair shaft (g). In order to facilitate the calculation of each volume, the model block was divided into three sections parallel to the skin surface. Section I extends from the skin surface to the epidermal–dermal junction. Section II goes from this junction to the end of the gap leaving the rest for section III. Volumes of a skin area was calculated for each section and subsequently added up to obtain the volume in the model skin block.

influence on the movement of the point of focus the series of images obtained were excluded as well.

2.2.4. Data analysis

Skin regions of interest were the stratum corneum, viable epidermis, dermis, gap, outer root sheath, cuticle and the hair shaft. The inner root sheath is not present in the infundibulum of the hair follicle and could therefore not be visualised. Using the Image J software, circular areas were marked being representative for a specific skin region and the average intensity was measured. With slight modifications to the previously published relative quantification method [21], relative fluorescence values (F_{rel}) and relative accumulation values (f_{acc}) were determined from these average intensities as described below. In order to be able to calculate these accumulation values, a model skin block measuring 400 μm on all three sides (Fig. 1C) was taken to calculate the appropriate volumes of the various skin parts. For the determination of the volumes, the skin block was divided into three horizontal sections (Fig. 1B). The first section extended from the stratum corneum up to the epidermal–dermal junction and the second up to the point where the gap ends. The basic dimensions of key elements within the model skin block were obtained from the time series images: hair shaft (diameter = 49.4 μm), gap opening (diameter = 121.5 μm), gap (depth = 222.8 μm), upper outer root sheath (width = 49.0 μm), lower outer root sheath (width = 33.1 μm), cuticle (width = 2.8 μm), stratum corneum (depth = 9.6 μm) and viable epidermis (depth = 76.8 μm). The mean number of the hair follicles (160 per cm^2) was counted and also included into the model skin block. The obtained volumes are summarised in Table 1.

The calculation of the relative accumulation in a time resolved experiment is similar to the previous published method to determine the relative accumulation [21] in a static experiment. Briefly, for every selected area the average fluorescence intensity (I_{av}), the analysed area (A) in μm^2 and the number of pixels (n_{pix}) are obtained by the Image J software. The intensity density (ID) is the fluorescence intensity per unit area and is calculated as follows (Eq. (1)).

$$ID = I_{av} \cdot n_{pix}/A \quad (1)$$

The relative intensity density ($ID_{rel\ i}$) of each skin part (i) expresses the relative distribution of the fluorescence in the images without including the equivalent volumes of each skin part with ID_{tot} being the sum of all ID_i's (Eq. (2)). That means the ID_{rel} is a means of comparing the fluorescence distribution assuming the same volume for all skin areas.

$$ID_{rel\ i} = ID_i/ID_{tot} \cdot 100\% \quad (2)$$

Table 1
Volume and relative volume of various skin areas in a model skin block of 400 μm side length

	Volume (V) (10^6 μm^3)	Relative volume (V_{rel}) (%)
Stratum corneum	1.56	2.44
Viable epidermis	12.19	19.05
Dermis	48.99	76.55
Gap total	0.21	0.33
Gap section I	(0.13)	(0.20)
Gap section II	(0.08)	(0.13)
Outer root sheath	0.80	1.25
Cuticle total	0.05	0.07
Cuticle section I	(0.01)	(0.01)
Cuticle section II/III	(0.04)	(0.06)
Hair shaft	0.20	0.31
Total skin block	64.00	100.00

The density of hair follicles was determined (160 follicles per cm^2) and incorporated in the skin model. The volumes of the gap and the cuticle of section I and II/III are already incorporated in the total volume of the equivalent skin part and are therefore not part of the total skin block as indicated by the brackets.

Now the actual volume of each skin part (Table 1) is included into the calculation by multiplying the $ID_{rel\ i}$ by the volume of each skin part (V_i). The relative fluorescence distribution ($F_{rel\ i}$) in the model skin block is obtained by dividing this product by the sum of all $ID_{rel\ i} \cdot V_i$ (Eq. (3)).

$$F_{rel\ i} = \frac{ID_{rel\ i} \cdot V_i}{\sum(ID_{rel\ i} \cdot V_i)} \quad (3)$$

The relative fluorescence values give access to distribution changes of the fluorescence in the model skin block; however, not to changes in the relative accumulations. For this reason the relative accumulation factor (f_{acc}) was introduced. This factor expresses the actual relative fluorescence compared to the relative fluorescence at homogeneous distribution. The latter is equal to the relative volumes ($V_{rel\ i}$) of each skin part (Table 1, Eq. (4)). Therefore the $f_{acc\ i}$ is independent of the volume of each skin part and is a

better means to compare accumulation changes within the skin than the $F_{rel\ i}$ values.

$$f_{acc\ i} = \frac{F_{rel\ i}(\text{in } \%)}{V_{rel\ i}(\text{in } \%)} \quad (4)$$

If the relative distribution value ($F_{rel\ i}$) is higher than the equal distribution value (expressed in $V_{rel\ i}$ [%]), i.e. a value for $f_{acc\ i}$ above 1, label accumulation in the selected part is present.

The F_{rel} values were calculated for the non-follicular (stratum corneum, epidermis, dermis), the gap and the follicular (outer root sheath, cuticle, hair shaft) area while the f_{acc} values were determined for all of the mentioned areas separately.

3. Results

3.1. On-line diffusion

Fig. 2A depicts images at a 1.5-h time interval of the diffusion of Bodipy® FL C_5 into fresh unfixed human scalp skin combined with the quantification of the fluorescence in time (Fig. 2B). Directly after application (10 min) of the dye, the label is only present in the donor phase. Penetration into the skin occurs via the whole surface however in the initial diffusion process, interestingly, the deepest regions are reached fastest via the gap (Fig. 2A, 1 h and 40 min) of the hair follicle. After 3 h the cuticle shows intense staining as well. Fig. 2B shows that fluorescence intensity increases fastest in the cuticle and the upper gap. The lower gap reveals the fastest increase of fluorescence intensity of the skin parts situated below the epidermal–dermal junction. In all other skin parts of the deeper skin regions (lower cuticle, dermis and hair shaft) a slow increase of fluorescence intensity is observed. As the diffusion process proceeds the intensity of the gap decreases together with a reduction in fluorescence intensity in the donor phase while the intensity of the cuticle is not decreasing yet (Fig. 2A, B). At later time points, also the intensity of the cuticle decreases. Staining of the epidermis increases in the initial phase and remains nearly constant throughout the diffusion process with slight decrease at late time points as seen in the images and the figure. The outer root sheath cannot be distinguished from the surrounding tissue in the initial period of the diffusion process, however the outer root sheath is stained at later time points.

A higher magnification of the gap area of the hair follicle after the on-line time series revealed more detailed information on the location of the fluorophore (Fig. 3). At the skin surface (Fig. 3D) strong staining of the top layers of the stratum corneum are observed with less labelling of the same structure a few micrometers deeper (mainly in the intercellular regions). In the epidermis, nuclei appear as dark areas with indications of staining of their nucleus membrane whereas the cytosol shows homogeneous staining. The dermis contains little label. Fig. 3B displays an enlarged hair shaft where cells start to form a close contact with the hair shaft. The lower left hand corner (closest to the surface) shows straight outlines while the upper right hand corner (deeper in the skin) reveals less sharp outlines of the hair shaft. Close to the cross-sectional surface where scattering and absorption of the fluorescence is lowest, details of the outer root sheath are visible (Fig. 3C). At the end of the experiment the outer root sheath shows stronger labelling than the dermis and the hair gap with similar stained features as the epidermis. However absolute intensities of skin areas of two different enlargements cannot be compared quantitatively.

3.2. Relative fluorescence values

The fluorescence intensity of the images has been measured every half-hour and analysed for several skin areas. In order to gain insight in the relative distribution of the fluorescence in the follicular region within the model skin block, a distinction has been made between the non-follicular part, the follicular part and the gap. From Fig. 4, it is clear that the initial relative fluorescence values after 10 min show high variations in the follicular and the non-follicular region. However, already after 40 min these variations are strongly reduced. The F_{rel} values reveal that the relative fluorescence in the non-follicular part does not drop below 97.5% in a time period from 0 up to 16 h. However, a decrease of the relative contribution of the non-follicular part in time is observed. Consequently, the total contribution of the area of the hair follicle and gap does not exceed 2.5%. Interestingly, a difference is observed for these two skin regions. In

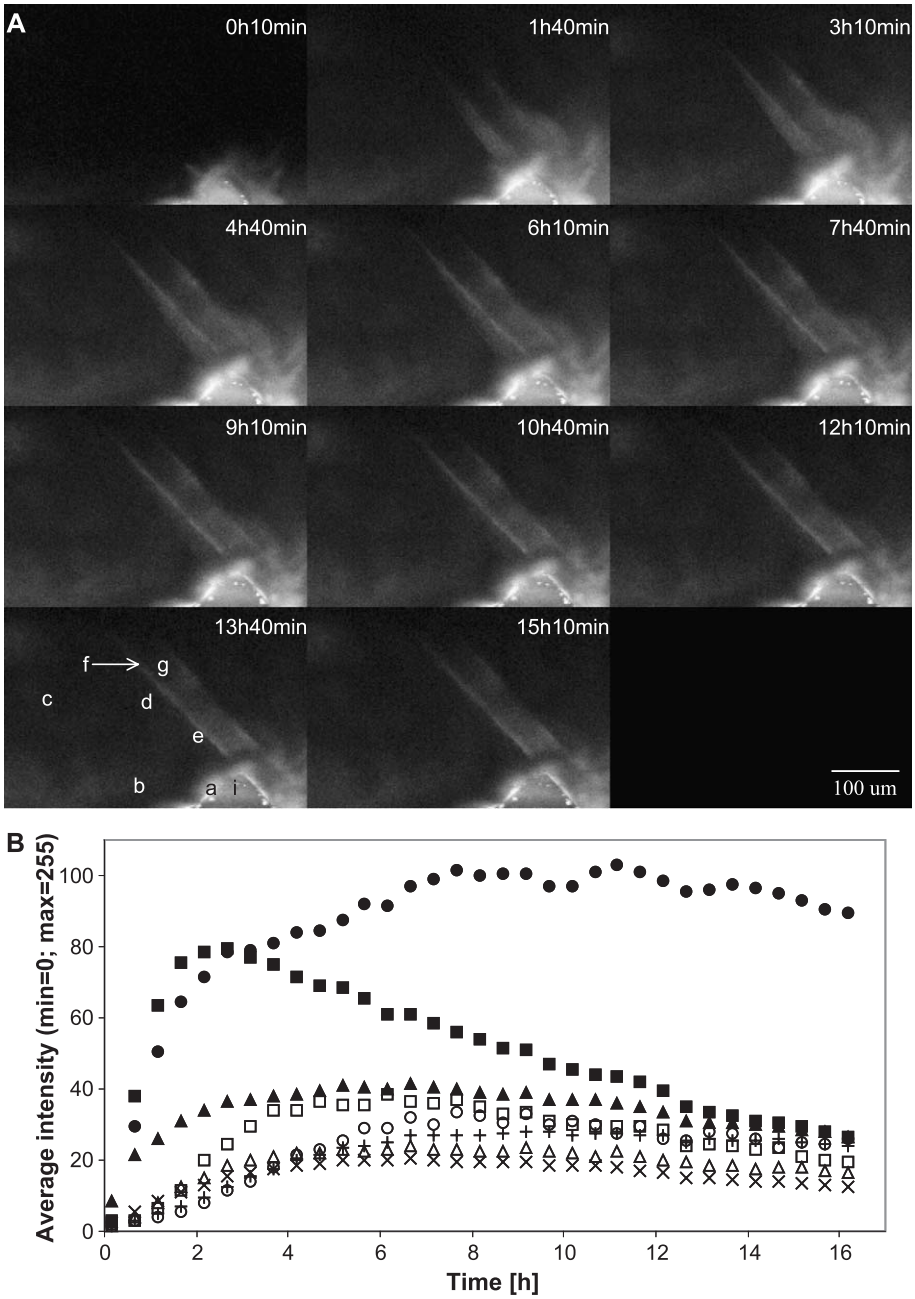

Fig. 2. On-line visualisation (CLSM) of the diffusion of 0.1 mg/ml Bodipy® FL C_5 applied in citric acid buffer pH 5.0. Changes in distribution in a cross-sectional view can be followed over time by use of a newly developed on-line visualisation device. (A) CLSM images are depicted in a 1-h and 30-min time interval starting 10 min after application. (a) Stratum corneum, (b) viable epidermis, (c) dermis, (d) outer root sheath, (e) gap, (f) cuticle, (g) hair shaft and (i) donor phase. (B) Displays the average fluorescence intensity analysed by Image J of the selected areas over 16 h. Upper gap (■), lower gap (□), upper cuticle (●), lower cuticle (○), outer root sheath (Δ), hair shaft (+), epidermis (▲) and dermis (×).

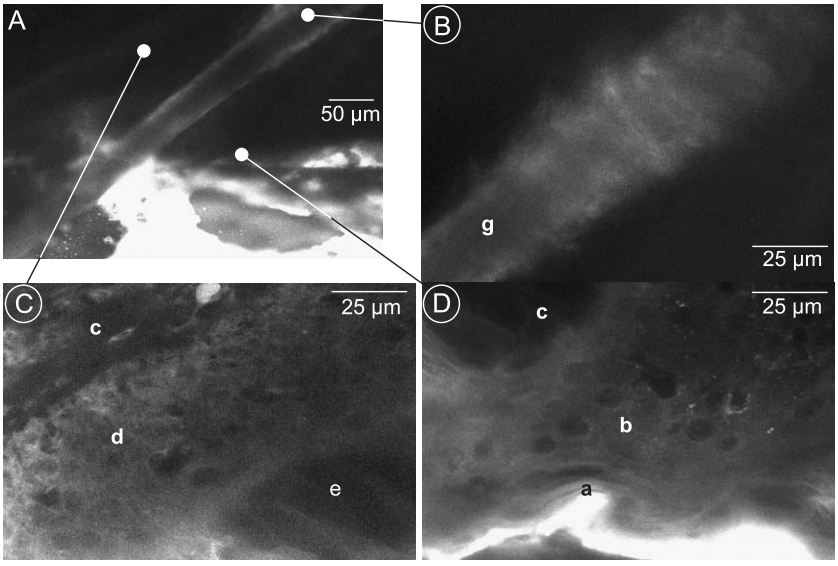

Fig. 3. 0.1 mg/ml Bodipy® FL C_5 applied in citric acid buffer pH 5.0 in a newly developed on-line visualisation device. Distribution of Bodipy® FL C_5 visualised by CLSM in a cross-sectional view of human scalp skin after 16 h on-line visualisation. (A) Last image of an on-line series visualised with a PlanApo 20 objective. Images (B–D) display details of image (A) indicated by lines using a PlanApo 60 objective closer to the cross-sectional cutting surface. (B) Enlargement of the hair shaft (g) at the point where a tighter contact is formed with the skin, (C) enlargement of the area of the outer root sheath (d), dermis (c) and gap (e), (D) focus on the stratum corneum (a), epidermis(b), and dermis.

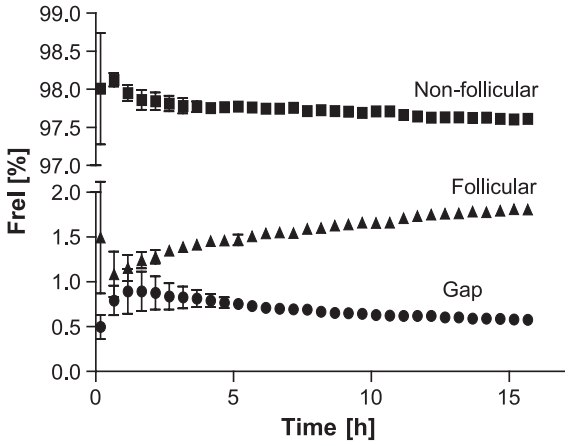

Fig. 4. Relative fluorescence values of Bodipy® FL C_5 (saturated solution in citric acid buffer pH 5.0) in a model skin cube of with side length of 400 µm. The values were obtained after quantification of the average fluorescence intensity of selected skin areas in the CLSM on-line time series using the Image J software. Subsequently the average intensities had to be transformed as explained in Section 2.2. Depicted values are averages of $n=3$ of the non-follicular (■), the follicular (▲) and the gap region (●).

the initial stage of diffusion the relative contribution of the gap to the total fluorescence intensities in the model skin block increases, followed by a decrease after 2 h. In the follicular region the opposite is observed where an initial drop of the relative fluorescence contribution is followed by a continuous increase. After 2 h the relative fluorescence contribution in the hair follicle is significantly higher than in the gap with $P<0.05$. Due to the absence of fluorescence immediately after the start of the diffusion experiment and the larger volume of the follicular region compared to the gap, the rather high F_{rel} is observed for the follicular region.

3.3. Relative accumulation values

To obtain information regarding the actual accumulation in certain skin parts, the relative accumulation values were determined in various parts of the skin and of the hair follicle (Fig. 5, donor 1–3). This figure shows that f_{acc} values between the donors vary to a certain extent. However the change in the f_{acc} values within time and within one skin area is similar.

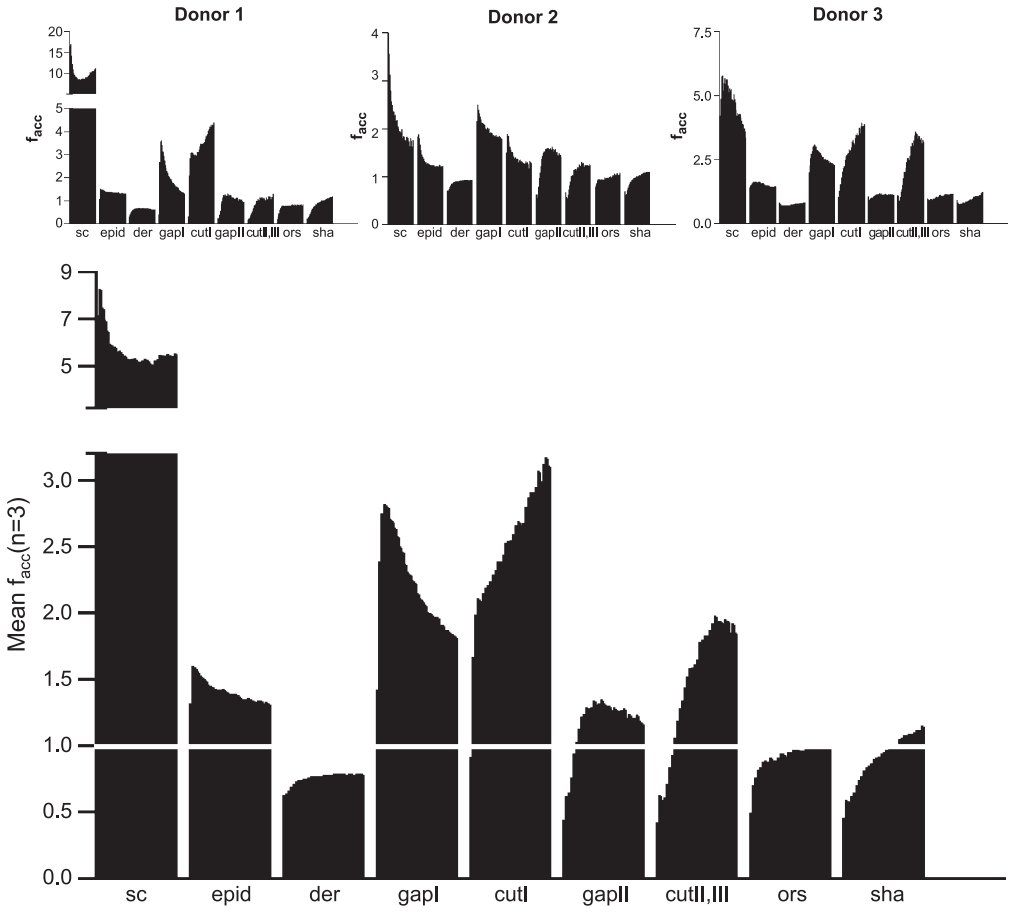

Fig. 5. Relative accumulation factors (f_{acc}) of three different donors (donor 1–3) and their average (mean f_{acc}) for selected skin regions in the previously mentioned sections of the model skin block (Fig. 1). The f_{acc} was determined for stratum corneum (sc), epidermis (epid), dermis (der), upper gap (gapI) and the upper cuticle in section I (cutI). Furthermore it was determined for the lower gap in section II (gapII), the lower cuticle representative of sections II/III (cutII, III), outer root sheath (ors) and hair shaft (sha). For each skin area f_{acc} values are displayed as bars in a 30 min time interval starting 10 min after application of a saturated Bodipy® FL C_5 solution in citric acid buffer up to 16 h. A white line indicates the f_{acc} value of one. Values >1 imply accumulation in that specific area with regard to homogeneous distribution.

Summarising all three donors the overall change in the relative accumulation of the fluorescence is provided in Fig. 5. In the stratum corneum the highest f_{acc} is observed in the initial diffusion period and decreases in the first hours to reach a constant level. In the epidermis, a similar trend is observed with two differences. In the first hour, the f_{acc} value increases, after which the f_{acc} subsequently decreases, but to a lesser extent than in the stratum corneum. In the dermis all relative accumulation values in time are below a value of 1 indicating that this is a skin area with low fluorescence intensity. An increase is observed in the first hours reaching a constant value during the remaining diffusion process. Focussing on the area of the hair follicle starting with the gap close to the surface, a sudden increase (twice the initial value) within the first 1.5 h of the f_{acc} value is determined. After reaching this maximum value, a fast decrease is observed. However, the relative accumulation values in the lower part of the gap show another trend in time. The initial increase of the f_{acc} is threefold, but extends over 7–8 h. However, the overall f_{acc} values are lower than the values calculated for the upper part of the gap. After 7–8 h only a slight decrease occurs with time in the lower part of the gap. Focussing at the hair cuticle, which is in direct contact with the gap, a

different observation is made. Overall the lower part of the cuticle reaches lower f_{acc} values than the upper part of the cuticle indicating a fluorescent intensity gradient. This gradient remains for the remaining diffusion period. In the upper as well as lower part of the cuticle, f_{acc} values increase fourfold compared to the initial value, however, the time schedules at which this fourfold increase is reached is completely different. The increase in the upper part of the cuticle is very fast in the first 1.5 h and slows slightly down in the following time period. In the lower part of the cuticle, the increase is more gradually reaching a constant level after 12 h diffusion. In the outer root sheath of the infundibulum and in the hair shaft f_{acc} values are very low. Within the outer root sheath after a moderate initial increase, a constant value of 1 is reached. In the hair shaft the increase is continuous. Overall in the initial period of the diffusion process relative accumulation values above 1 are only determined for the stratum corneum and the upper gap. At later time points the stratum corneum, viable epidermis, the upper/lower gap and the upper/lower cuticle reveal f_{acc} values >1 as well.

4. Discussion

4.1. On-line diffusion

Previously Hoogstraate et al. [24] have visualised on-line diffusion in buccal tissue. In that study, the size donor and acceptor compartments varied substantially since the compartments were created solely by dental clay. Furthermore diffusion processes into the buccal tissue were visualised for less than 2 h. Since no stratum corneum is present in the buccal tissue fast diffusion was expected and a short time period was sufficient. However in the case of intact skin, where the diffusion is much slower, the diffusion process has to be examined over a longer period of time. We were able to visualise diffusion processes over time periods as long as 16 h in a 30-min time interval. Acquisition intervals of 2 min can be achieved if necessary. In the present construction the donor and acceptor phases are static without flow-through mechanism to replace either of the solutions. Very recent studies have shown the possibility of creating flow-through mechanisms for either compartment thereby ensuring infinite penetrant concentration in the donor phase and sink conditions in the acceptor phase. This will be an aim of our future research.

From the images obtained on-line it is obvious that the gap presents a low resistance for the diffusion of a lipophilic label from an aqueous donor solution into hairy skin. The lipophilic nature of the sebum paired with an absence of a tight cell structure such as present in the stratum corneum provides a favourable environment for the penetration of the Bodipy® dye. After entering the gap, the cuticle of the hair shaft appears to have a high affinity for the applied dye. Even after the fluorescence intensity of the gap decreases, the cuticle retains the fluorophore for a longer time period. This implies that the cuticle has a high up-take of the fluorophore, however it does not release the dye at the same speed in the initial time period.

In the donor phase, the gap and at a later stage in the diffusion process also in the cuticle, a decrease of fluorescence intensity is observed. Photobleaching has been tested previously. With more scans than used in this experiment only weak photobleaching was observed which could not be accounted for the degree of fluorescence decrease observed in our images. Furthermore photobleaching would be expected to occur simultaneously in the gap and the cuticle instead of shifted in time like observed in our time series. Therefore, it is more likely for the dye to diffuse most likely further into deeper skin regions along the concentration gradient.

4.2. Relative fluorescence values

It is generally known that the surface area of the hair follicle is 0.1–1% of the total skin surface [25]. Recently it has been pointed out, that regional differences in the follicular openings are present [26]. In our study, this results in a relative fluorescence of 2.4% in the follicular region (gap and hair follicle) of the model skin block. Assuming that the diffusion coefficient in the hair follicle is of a similar order of magnitude as in the inter-follicular area one might conclude that for this dye the overall contribution of the follicular region to the transport through the skin might therefore be limited. Compared to in vivo studies where the vascularisation of the hair follicle is intact, in vitro studies might underestimate the contribution of the hair follicle to the overall transport

due to the lack of blood circulation and the decreased follicular opening. At the same time hair follicles occur in different stages of growth and activity, which might also have an influence on the penetration behaviour [27]. However their influence is not investigated in this study.

Although the contribution of the follicular route to the overall transport is limited for this dye, this transport route might be of importance to reach deeper skin layers such as the dermis. This topic is subject of future studies.

4.3. Relative accumulation values

Focussing first on the f_{acc} values of the individuals it can be concluded, that the skin of donor 2 reveals the least variation of f_{acc} between different skin areas. The fluorescence intensities of the time series of donor 2 were very low reaching only 17% of the maximum intensities detectable with the settings we used. This reduces the sensitivity for changes in intensity. This implies that the in pilot experiments determined optimal settings for the on-line detection of the label were excellent for donor 1 and 3, but less suitable for donor 2. This phenomenon stresses also the high variability of skin permeability particularly in scalp skin, which has also been observed by another group [28]. Scalp skin is more exposed to various treatments like fixatives, colouring agents, cleansing and conditioning products which might have an effect on the barrier function. Additionally differences between individuals are expected to be higher than for normal skin due to different styling behaviour.

Initially the increase in relative accumulation factors is strongest in the top section of the gap and the upper part of the cuticle. This indicates that the diffusion of the dye is dominating in these regions at early time points. The fact that the stratum corneum has a very high accumulation factor can be attributed to a certain amount of label, which is attached to the skin surface. Since Bodipy® FL C_5 is a lipophilic dye (log P 2.5 at pH 5.0) of a small size, penetration is expected to be relatively high. This has been shown previously for a buffer phase containing 30% ethanol [29] or 8% surfactants [30]. Our finding is therefore in agreement with the model of Scheuplein [31]. He stated that in the initial period the follicular pathway is of greater importance for the diffusion process than the pathway via the skin surface especially for a substance penetrating the stratum corneum very slowly. However from our studies it is clear that diffusion of this particular dye occurs via the stratum corneum and via the follicular duct. In some regions of the deeper skin layers such as the outer root sheath, the dermis and the hair shaft the f_{acc} increase slower than other regions in the same depth such as the lower gap and the lower cuticle. This implies that label in the deeper parts of the cuticle can originate from the hair canal and from the upper cuticle, but not from the outer root sheath, dermis or hair shaft. This is also supported by the fact that the f_{acc} values of the outer root sheath, the dermis and the hair shaft do not reach values above 1 implying that no accumulation is present. The stratum corneum is the main barrier at the surface and the upper part of the gap where it thins out up to a depth of approximately 200 μm [32]. This is in agreement with the strong labelling of the gap and the cuticle.

The results of the present experiments strongly indicate that the high amount of fluorophore, which is present in the hair duct, diffuses into the cuticle. This is based on the fact that the relative accumulation in the cuticle follows with a certain delay the development of the fluorescence in the gap. This does not exclude diffusion from other parts such as along the hair shaft and from the outer root sheath of the infundibulum to the cuticle or any diffusion from the gap into the outer root sheath.

5. Conclusion

On-line CLSM is a recently developed tool to visualise the diffusion of a dye in a cross-sectional view of fresh unfixed piece of skin including subcutaneous fat. From these studies we conclude that this technique can visualise the diffusion of a dye into the upper hair follicle at different time points. Thereby the two disadvantages of (i) increased scattering and absorption in deeper layers of the skin from conventional depth scans and (ii) the limitation in depth due to optical sectioning is avoided. We can conclude that a lipophilic dye penetrates at early time points via the stratum corneum and the gap. Since the diffusion into the gap is fast and reaches deeper skin layers, we conclude that the diffusion resistance for a lipophilic compound is lower in the gap than in the stratum

corneum/epidermis of the same thickness. From the gap label diffuses into the cuticle where it accumulates. However, it cannot be excluded that diffusion also takes place to some extent in the other directions as well. Since the hair follicle is highly vascularised, the follicular contribution to the overall transport in vivo might be underestimated. For local delivery the here presented method is of great value to study the influence of parameters on the accumulation in regions of interest such as hair follicles and sweat ducts. Deeper skin regions e.g. sebaceous gland, sweat gland and non-infundibulum area of the hair follicle will be examined in the future.

Acknowledgements

We would like to thank Jan Janssen and Henk Verpoorten for the co-operation in the development of the on-line diffusion cell. Furthermore we acknowledge Unilever Research, Port Sunlight, UK for financing this project.

References

[1] A.C. Lauer, L.M. Lieb, C. Ramachandran, G.L. Flynn, N.D. Weiner, Transfollicular drug delivery, Pharm. Res. 12 (1995) 179–186.
[2] E. Touitou, V.M. Meidan, E. Horwitz, Methods for quantitative determination of drug localized in the skin, J. Control. Release 56 (1998) 7–21.
[3] P. Corcuff, G.E. Pierard, Skin imaging: state of the art at the dawn of the year, Curr. Problem Dermatol. 26 (1998) (2000) 1–11.
[4] P.J. Caspers, G.W. Lucassen, G.J. Puppels, Combined in vivo confocal Raman spectroscopy and confocal microscopy of human skin, Biophys. J. 85 (2003) 572–580.
[5] P. Corcuff, G. Gonnord, G.E. Pierard, J.L. Leveque, In vivo confocal microscopy of human skin: a new design for cosmetology and dermatology, Scanning 18 (1996) 351–355.
[6] A.J. Hoogstraate, S. Senel, C. Cullander, J. Verhoef, H.E. Junginger, H.E. Bodde, Effects of bile salts on transport rates and routes of FITC-labelled compounds across porcine buccal epithelium in vitro, J. Control. Release 40 (1996) 211–221.
[7] B.R. Masters, G. Gonnord, P. Corcuff, Three-dimensional microscopic biopsy of in vivo human skin: a new technique based on a flexible confocal microscope, J. Microsc. 185 (1997) 329–338.
[8] S. Senel, A.J. Hoogstraate, F. Spies, J.C. Verhoef, H.E. Junginger, H.E. Bodde, Visualization of enhancing effects of bile salts on buccal penetration, Eur. J. Morphol. 31 (1993) 35–41.
[9] O. Simonetti, A.J. Hoogstraate, W. Bialik, J.A. Kempenaar, A.H.G.J. Schrijvers, H.E. Bodde, M. Ponec, Visualization of diffusion pathways across the stratum corneum of native and in vitro-reconstructed epidermis by confocal laser scanning microscopy, Arch. Dermatol. Res. 287 (1995) 465–473.
[10] N.G. Turner, R.H. Guy, Visualization and quantitation of iontophoretic pathways using confocal microscopy, J. Invest. Dermatol. Symp. Proc. 3 (1998) 136–142.
[11] D. Aghassi, R.R. Anderson, S. Gonzalez, Confocal laser microscopic imaging of actinic keratoses in vivo: a preliminary report, J. Am. Acad. Dermatol. 43 (2000) 42–48.
[12] D. Aghassi, E. Gonzalez, R.R. Anderson, M. Rajadhyaksha, S. Gonzalez, Elucidating the pulsed-dye laser treatment of sebaceous hyperplasia in vivo with real-time confocal scanning laser microscopy, J. Am. Acad. Dermatol. 43 (2000) 49–53.
[13] D. Aghassi, R.R. Anderson, S. Gonzalez, Time-sequence histologic imaging of laser-treated cherry angiomas with in vivo confocal microscopy, J. Am. Acad. Dermatol. 43 (2000) 37–41.
[14] C. Bertrand, P. Corcuff, In vivo spatio-temporal visualization of the human skin by real-time confocal microscopy, Scanning 16 (1994) 150–154.
[15] P. Corcuff, J.L. Leveque, In vivo vision of the human skin with the tandem scanning microscope, Dermatology 186 (1993) 50–54.
[16] P. Corcuff, C. Bertrand, J.L. Leveque, Morphometry of human epidermis in vivo by real-time confocal microscopy, Arch. Dermatol. Res. 285 (1993) 475–481.
[17] S. Gonzalez, G. Rubinstein, V. Mordovtseva, M. Rajadhyaksha, R.R. Anderson, In vivo abnormal keratinization in Darier–White's disease as viewed by real-time confocal imaging, J. Cutan. Pathol. 26 (1999) 504–508.
[18] M. Rajadhyaksha, R.R. Anderson, R.H. Webb, Video-rate confocal scanning laser microscope for imaging human tissues in vivo, Appl. Opt. 38 (1999) 2105–2115.
[19] W.M. White, M. Rajadhyaksha, S. Gonzalez, R.L. Fabian, R.R. Anderson, Noninvasive imaging of human oral mucosa in vivo by confocal reflectance microscopy, Laryngoscope 109 (1999) 1709–1717.
[20] C. Cullander, Light microscopy of living tissue: the state and future of the art, J. Invest. Dermatol. Symp. Proc. 3 (1998) 166–171.
[21] Y.Y. Grams, J.A. Bouwstra, A new method to determine the distribution of a fluorophore in scalp skin with focus on hair follicles, Pharm. Res. 19 (2002) 350–354.
[22] M.E.M.J. Meuwissen, J. Janssen, C. Cullander, H.E. Junginger, J.A. Bouwstra, A cross-section device to improve visualization of fluorescent probe penetration into the skin by confocal laser scanning microscopy, Pharm. Res. 15 (1998) 352–356.
[23] Y.Y. Grams, L. Whitehead, G.L. Li, P. Cornwell, J.A. Bouwstra, On-line visualisation of dye diffusion in fresh unfixed human skin, Pharm. Res. 21 (2004) 851–859.
[24] A.J. Hoogstraate, C. Cullander, J.F. Nagelkerke, F. Spies, J. Verhoef, A.H.G.J. Schrijvers, H.E. Junginger, H.E. Bodde, A novel in-situ model for continuous observation of transient drug concentration gradients across buccal epithelium at the microscopical level, J. Control. Release 39 (1996) 71–78.

[25] H. Schaefer, T.E. Redelmeier, Skin Barrier, Karger AG, Basel, 1996.
[26] N. Otberg, H. Richter, H. Schaefer, U. Blume-Peytavi, W. Sterry, J. Lademann, Variations of hair follicle size and distribution in different body sites, J. Invest. Dermatol. 122 (2004) 14–19.
[27] J. Lademann, N. Otberg, H. Richter, H.-J. Weigmann, U. Lindemann, H. Schaefer, W. Sterry, Investigation of follicular penetration of topically applied substances, Skin Pharm. Appl. Skin Phys. 14 (2001) 17–23.
[28] T. Ogiso, T. Shiraki, K. Okajima, T. Tanino, M. Iwaki, T. Wada, Transfollicular drug delivery: penetration of drugs through human scalp skin and comparison of penetration between scalp and abdominal skins in vitro, J. Drug Target. 10 (2002) 369–378.
[29] Y.Y. Grams, J.A. Bouwstra, Penetration and distribution of three lipophilic probes in vitro in human skin focusing on the hair follicle, J Control. Release 83 (2002) 253–262.
[30] Y.Y. Grams, S. Alaruikka, L. Lashley, J. Caussin, L. Whitehead, J.A. Bouwstra, Permeant lipophilicity and vehicle composition influence accumulation of dyes in hair follicles of human skin, Eur. J. Pharm. Sci. 18 (2003) 326–329.
[31] R.J. Scheuplein, Mechanism of percutaneous absorption. II. Transient diffusion and the relative importance of various routes of skin penetration, J. Invest. Dermatol. Symp. Proc. 48 (1967) 79–88.
[32] G.F. Odland, Skin, in: R.O. Greep (Ed.), Histology, McGraw-Hill Company, New York, 1966.